POWER GRID IMPEDANCE TRACKING WITH UNCERTAINTY ESTIMATION USING TWO STAGE WEIGHTED LEAST SQUARES

Dariusz Borkowski, Szymon Barczentewicz

AGH University of Science and Technology, Department of Measurement and Electronics, al. A. Mickiewicza 30, 30-059 Kraków, Poland
(✉ borkows@agh.edu.pl, +48 12 617 28 41, barczent@agh.edu.pl)

Abstract

The paper presents a new method for simultaneous tracking of varying grid impedance and its uncertainty bounds. Impedance tracking consists of two stages. In the first stage, the actual noise estimate is obtained from least squares (LS) residua. In the second stage, the noise covariance matrix is approximated with the use of residual information. Then weighted least squares (WLS) method is applied in order to estimate impedance and background voltage. Finally uncertainty bounds for impedance estimation are computed. The robustness of the method has been verified using simulated signals. The proposed method has been compared to sliding LS. The results have shown, that the method performs much better than the LS for all considered cases, even in the presence of significant background voltage variations.

Keywords: power system, utility impedance tracking, uncertainty estimation.

1. Introduction

Central power plants are still dominant electric energy sources in most countries. However, increasing power demand and more frequent failures of power systems have forced electric engineers to consider new solutions like distributed power generation as well as to provide continuous grid monitoring and control. Simultaneous generation by many small energy sources (photovoltaic panels, wind turbines, etc.) as well as operation of sensitive loads require continuous monitoring of grid impedance at the point of common coupling (PCC) [1]. Such information allows us to detect faults and sudden changes in power demand. The nature of time variations of grid impedance can also be used for verification of flicker source localization methods, like the one presented in [2].

A number of methods for grid impedance measurement have been developed over the last 20 years [3]. These can be generally classified as invasive or non-invasive [4, 5]. Invasive methods rely on controlled disturbance/excitation in a form of current pulses injection [6, 7] or utilization of converter switching noise [8, 9]. Thus they usually offer higher accuracy, when compared with non-invasive ones. On the other hand, their use is limited to low voltage grids and the locations where the power electronic converters are installed. Continuous tracking of time varying impedance using invasive methods may be problematic, especially in grids of medium or high voltage levels, due to the requirement of continuous, high-power, controlled disturbance [10]. Non-invasive methods are better suited for impedance tracking, because they use only natural customer side variability as the source of excitation [11, 12, 13].

The biggest disadvantage of non-invasive methods is the fact, that they do not ensure the credibility of the result, because they rely on a natural, uncontrollable variability of a grid. Moreover, the uncertainty of the results is a varying quantity due to varying properties of the excitation and the impact of background voltage variations. Therefore, the estimation of instantaneous uncertainty of impedance tracking results is a desired feature of a tracking methods.

The authors propose a new method for simultaneous tracking of varying grid impedance and its uncertainty bounds.

2. Power system model

The grid seen from the PCC can be modelled as Thevenin or Norton circuit [13], the former being usually used to model the grid side containing fundamental frequency voltage source. One-phase Thevenin/Norton equivalent power grid model shown in Fig. 1 is considered in the paper.
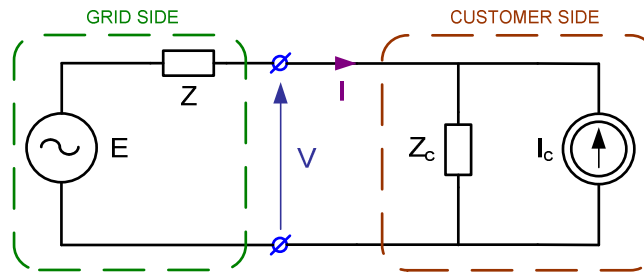

Fig. 1. Power system model.

According to the model shown in Fig. 1, complex voltage V for a given frequency (e. g. fundamental one) can be computed as:

$$V = E - IZ, \tag{1}$$

where I is complex PCC current, Z is complex impedance of the grid to be estimated and E is complex background voltage of equivalent source.

The only measurable quantities are voltage V and current I. Due to unknown value of E, the estimation of the unknown Z requires solving the system composed of at least two equations (1) containing two different pairs V and I. The source of excitation is the variation of the customer side parameters, i.e. Z_C and/or I_C, which impacts values V and I. Assuming invariance of Z and E during the experiment and having sufficient number of complex data samples of V and I containing load variations, one can estimate Z and E using the LS method [13].

Assuming that the measurement noise is a) complex normal i.i.d (independent, identically distributed), b) additive to the output signal of the object (the voltage V in this case), c) not correlated with the input (the current I in this case), the LS is minimum variance unbiased (MVU) estimator [14].

The biggest problem is that such assumptions are hard to meet in a real power system. Variations of impedance Z are rather slow and periodical [13]. Magnitude of source voltage E can change frequently, usually in a step manner, which can result from e.g. automatic voltage regulation (AVR) systems [5]. All these facts violate the assumptions of the MVU LS estimator.

Complex samples of V and I are usually obtained from time domain signals using Discrete Fourier Transform (DFT) [15, 16]. DFT may be computed recursively using sliding window techniques [17]. Main problem associated with computing DFT of power grid signals is its spectral leakage resulting from varying fundamental frequency of the grid. In order to avoid the leakage, sampling rate has to be synchronized with the actual voltage frequency, prior to the DFT computation. It can be realized by means of hardware sampling synchronization [18, 19] or software resampling methods [20, 21, 22]. In case of nonsynchronously sampled signals, what is common in phasor measurement units (PMUs), interpolated DFT methods can be used [23]. There are also adaptive filtering methods, which allow for direct calculation of leakage-free complex samples of V and I from nonsynchronously sampled time domain signals like Kalman filtering [24, 25] or phase locked loop (PLL) based [26].

3. The proposed Algorithm

Assuming two complex unknown quantities Z and E in (1) are fixed within single estimation, they can be calculated by solving at least two complex equations (1).

Output samples V contain unknown measurement errors ε. Thus, the equation (1) has to be extended by adding measurement noise (time index is dropped due to clarity):

$$V = -IZ + E + \varepsilon . \tag{2}$$

The reduction of noise impact is possible by collecting L measurements of V_l and I_l and solving a system of L equations:

$$\begin{cases} V_1 = -I_1 Z + E + \varepsilon_1 \\ V_2 = -I_2 Z + E + \varepsilon_2 \\ \quad \vdots \\ V_L = -I_L Z + E + \varepsilon_L \end{cases}, \tag{3}$$

which can be rewritten in a matrix form:

$$\mathbf{Y} = \mathbf{X}\boldsymbol{\Theta} + \boldsymbol{\varepsilon}, \tag{4}$$

where

$$\mathbf{Y} = \begin{bmatrix} V_1 \\ V_2 \\ \vdots \\ V_L \end{bmatrix}, \quad \mathbf{X} = \begin{bmatrix} -I_1 & 1 \\ -I_2 & 1 \\ \vdots & 1 \\ -I_L & 1 \end{bmatrix}, \quad \boldsymbol{\Theta} = \begin{bmatrix} Z \\ E \end{bmatrix}, \quad \boldsymbol{\varepsilon} = \begin{bmatrix} \varepsilon_1 \\ \varepsilon_2 \\ \vdots \\ \varepsilon_L \end{bmatrix}.$$

For now, we assume that errors vector $\boldsymbol{\varepsilon}$ contains only complex measurement noise $\boldsymbol{\varepsilon}$ resulting from sampling, quantization, electromagnetic interference, etc. According to the central limit theorem, the propagation of time domain measurement noise through relatively long DFT results in complex normal i.i.d noise [27]. Thus complex measurement noise variance σ_ε^2 can be evaluated on the basis of measurement system parameters, such as ADC resolution and range, measurement transformer ratio and DFT length.

The solution of (4) may not exist in a classical sense due to noise, but one can solve the system in the least squares sense by minimizing the sum of squared differences between the model and the object outputs [14]:

$$J(\boldsymbol{\Theta}) = (\mathbf{Y} - \mathbf{X}\boldsymbol{\Theta})^H (\mathbf{Y} - \mathbf{X}\boldsymbol{\Theta}) = \boldsymbol{\varepsilon}^H \boldsymbol{\varepsilon}, \tag{5}$$

where superscript ^{H} denotes conjugate transposition of a matrix. The LS solution of (4) is:

$$\hat{\boldsymbol{\Theta}} = (\mathbf{X}^H \mathbf{X})^{-1} \mathbf{X}^H \mathbf{Y}. \tag{6}$$

If the assumptions of the MVU LS estimator are fulfilled, then the uncertainty of the estimator can be evaluated in terms of its covariance matrix:

$$\mathbf{P} = (p_{i,j}) = \mathrm{cov}(\hat{\boldsymbol{\Theta}}) = \sigma_\varepsilon^2 (\mathbf{X}^H \mathbf{X})^{-1}, \tag{7}$$

which gives us values of variances (diagonal elements) and covariances (off-diagonal elements) of estimates $\hat{Z}$ and $\hat{E}$. Then standard uncertainty of $\hat{Z}$ is $u_c(\hat{Z}) = \sigma_{\hat{Z}} = \sqrt{p_{1,1}}$.

The estimation (6), (7) can be performed sequentially (sliding LS) in order to track slowly varying grid impedance together with its uncertainty. It can give accurate results under the assumption of local invariance of estimated parameters within estimation window.

Unfortunately, rapid variations of unknown background voltage E violate this assumption. They result in degrading impedance estimation accuracy and make its standard uncertainty $u_c(\hat{Z})$ strongly underestimated.

However, we can split background voltage E into two components: constant component E_-, which is a mean value of E within single data window, and varying (disturbing) component $E_\sim$, such that $E = E_\sim + E_-$. Then (2) can be rewritten in the following form:

$$V = -IZ + E_- + E_\sim + \varepsilon, \tag{8}$$

which modifies vector ε in the following way:

$$\boldsymbol{\varepsilon} = \begin{bmatrix} E_{\sim 1} + \varepsilon_1 \\ E_{\sim 2} + \varepsilon_2 \\ \vdots \\ E_{\sim L} + \varepsilon_L \end{bmatrix}. \tag{9}$$

The feature of LS estimator is that in case of variations of an estimated parameter within data window, its expected value is equal to the mean value of the parameter within data window [14]. This trait of LS estimator causes that using (4), in fact, we get $\hat{\boldsymbol{\Theta}} = \begin{bmatrix} \hat{Z} & \hat{E}_- \end{bmatrix}^T$. Thus, we can estimate disturbing component $E_\sim$ together with the noise ε in a form of residual vector:

$$\hat{\boldsymbol{\varepsilon}} = \mathbf{E}_\sim^{\wedge} + \boldsymbol{\varepsilon} = \mathbf{Y} - \mathbf{X}\hat{\boldsymbol{\Theta}}. \tag{10}$$

It can easily be shown that a step change in background voltage during single data window of L samples results in a complex bimodal distribution with much higher variance than the variance σ_ε^2 of noise ε only (see Fig. 2). A rough method for extending the underestimated uncertainty $u_c(Z)$ to a reasonable level could be the use sample variance $\mathrm{var}(\hat{\boldsymbol{\varepsilon}})$ of residual vector as the measurement errors variance σ_ε^2 in (7). However, it can also be noticed, that in case of a step change of $E_\sim$ consecutive samples of $\hat{\boldsymbol{\varepsilon}}$ are not strictly random and are strongly correlated with each other. This fact prompted us to use the weighted least squares (WLS) method as a second step of the proposed estimation procedure.
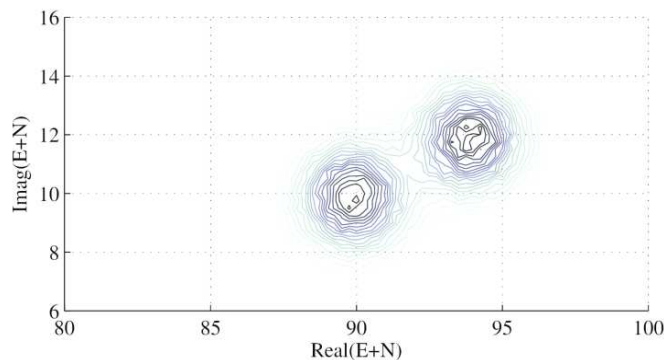

Fig. 2. Exemplary histogram of complex disturbing voltage E, containing step change from 90+j10 V to 94+j12 V located in the middle of data window length.

The WLS estimate of unknown parameters vector $\boldsymbol{\Theta}$ is given by:

$$\hat{\boldsymbol{\Theta}}_W = \left(\mathbf{X}^H \mathbf{W}^{-1} \mathbf{X} \right)^{-1} \mathbf{X}^H \mathbf{W}^{-1} \mathbf{Y}, \tag{11}$$

where $\mathbf{W}$ is a weighting matrix, which allows to put more emphasis on some measurements with respect to others, as well as to include information about the correlation between noise

samples. Optimal weighting matrix **W** is equal to unknown covariance matrix **C** of the noise ε [27]. The problem is that noise ε is unknown and its statistical properties can change with time between consecutive data windows of the sliding estimator because of nonstationary component $E_\sim$. Moving the analysis window along the data may cause unknown noise ε to be perceived as a correlation process, which is quite common e.g. in econometric analysis. It means that complex sample $\varepsilon_{l,m}$ with a fixed position l within m-th data window of the length L is correlated with sample $\varepsilon_{l,m+i}$ at the same position l in successive realizations $i = 1$, 2, ... of sliding data window. This phenomenon is depicted in Fig. 3.
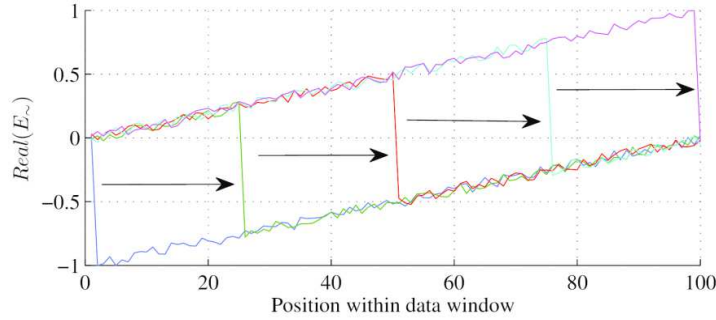

Fig. 3. Successive realizations of residual vector including step disturbance in $E_\sim$ while moving data window along the signals. Strong autocorrelation as well as zero mean of residuals is visible.

This fact allows us to approximate noise covariance matrix **C** in each realization from a single realization of residual vector $\hat{\varepsilon}$ as a matrix containing its shifted biased autocorrelation function estimates (Toeplitz structure) [28]:

$$\hat{\mathbf{C}} = \begin{bmatrix} \hat{a}_0 & \hat{a}_1 & \hat{a}_2 & \cdots & \hat{a}_{L-1} \\ \hat{a}_{-1} & \hat{a}_0 & \hat{a}_1 & \cdots & \hat{a}_{L-2} \\ \hat{a}_{-2} & \hat{a}_{-1} & \hat{a}_0 & \cdots & \hat{a}_{L-3} \\ \vdots & \vdots & \vdots & \ddots & \vdots \\ \hat{a}_{-L+1} & \hat{a}_{-L+2} & \hat{a}_{-L+3} & \cdots & \hat{a}_0 \end{bmatrix}, \tag{12}$$

where $\hat{a}_s$ is autocorrelation function estimate of residual vector $\hat{\varepsilon}$ for lag S. Due to zero mean of the residual vector $\hat{\varepsilon}$, autocorrelation estimate can be replaced with autocovariance estimate given as:

$$\hat{a}_s = \frac{1}{L} \sum_{l=0}^{L-1} \hat{\varepsilon}_l \hat{\varepsilon}_{l+s} . \tag{13}$$

Thanks to conjugate symmetry of autocorrelation function we can write $\hat{a}_{-s} = \hat{a}_s^*$. Such a form of weighting matrix **W** is a rough approximation of the actual noise covariance matrix (Fig. 4), but it can significantly improve tracking performance, which is shown in section 4.
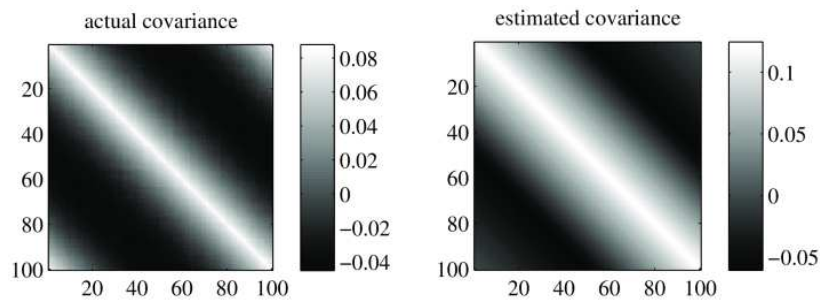

Fig. 4. Actual covariance matrix computed during pass of step disturbance $E_\sim$ through whole data window vs. covariance matrix estimated using (12). All axes scaled in values of lag s.

Finally, the uncertainty of the WLS estimator can be evaluated from its covariance matrix:

$$\mathbf{P}_W = \left(p_{Wi,j}\right) = \mathrm{cov}\!\left(\hat{\mathbf{\Theta}}_W\right) = \left(\mathbf{X}^H \mathbf{W}^{-1} \mathbf{X}\right)^{-1}. \tag{14}$$

Standard uncertainty of grid impedance estimation can be computed as:

$$u_c\!\left(\hat{Z}\right) = \sqrt{p_{W1,1}} \,. \tag{15}$$

Having grid impedance estimate $\hat{Z}$, as well as its standard uncertainty $u_c\!\left(\hat{Z}\right)$, its confidence interval is given by:

$$\hat{Z} \pm U\!\left(\hat{Z}\right) = \hat{Z} \pm k u_c\!\left(\hat{Z}\right), \tag{16}$$

where $U\!\left(\hat{Z}\right)$ is expanded uncertainty and k is an coverage factor, i.e. the number, by which the standard uncertainty should be multiplied in order to ensure that true impedance value lays within the confidence interval with given probability [29]. k value depends on probability distribution of a random variable $\hat{Z}$ as well as on requested confidence value. In general, the probability distribution of $\hat{Z}$ is unknown, but for most of the time, when no jumps of E exist within data window, it will be close to complex normal distribution. Thus, we choose $k = 2$, which gives confidence in case of normal distribution.

Summarizing, for n-th time instant grid impedance estimate $\hat{Z}(n)$ is computed with its confidence interval using L newest samples $V_{n-L+1},...,V_n$ and $I_{n-L+1},...,I_n$ in a following steps:

1. Vector $\hat{\mathbf{\Theta}} = \left[\hat{Z}\ \hat{E}\right]^T$ is calculated using (6).
2. Current noise realization $\hat{\boldsymbol{\varepsilon}}$ is estimated using (10).
3. Autocovariance estimates $\hat{a}_s$ of residua are calculated using (13) for $s = 0,...,L-1$.
4. Noise covariance matrix estimate $\hat{\mathbf{C}}$ is built as (12).
5. New estimates $\hat{\mathbf{\Theta}}_W$ of grid impedance and background voltage are calculated using WLS (11), substituting $\hat{\mathbf{C}}$ for $\mathbf{W}$.
6. Covariance matrix $\mathbf{P}_W$ of the WLS estimator is calculated using (14), for $\mathbf{W} = \hat{\mathbf{C}}$.
7. Standard uncertainty $u_C\!\left(\hat{Z}\right)$ is calculated using (15).
8. Confidence interval is calculated according to (16).

4. The results

The performance of the proposed algorithm was evaluated by means of tracking of simulated grid impedance variations in the Matlab environment. In order to show superiority of the algorithm, its results were compared to those obtained using the classic LS algorithm [13, 30].

4.1. Test cases

Simulation study included 16 test cases, each of which had different set of parameters describing grid side variations $E(n)$, $Z(n)$ and customer side variations $I_C(n)$, $Z_C(n)$, where n is time index. Each test consisted of simulation of a grid model from Fig. 1 and calculation of $N = 1440$ complex samples $V(n)$ and $I(n)$ of voltage and current at PCC, with the rate of one sample per minute. Grid model parameters $E(n)$, $Z(n)$, $I_C(n)$, $Z_C(n)$ were described by a general complex exponential form $M(n) \cdot e^{jA(n)}$, where $M(n)$ is the magnitude and $A(n)$ is the angle. Time variations of magnitudes and angles of $E(n)$, $Z(n)$, $I_C(n)$, $Z_C(n)$ were obtained by modulating base magnitudes M, M_Z, M_{I_C}, M_{Z_C} and base angles A_E, A_Z, A_{I_C}, A_{Z_C} respectively with deterministic or randomly varying terms.

Time variations of Z_n were obtained using deterministic sine and cosine terms. Time variations of $E(n)$, $I_C(n)$, $Z_C(n)$ were obtained using random series $R_{MZ_C}(n)$, $R_{MA_C}(n)$, $R_{MI_C}(n)$, $R_{ME}(n)$, $R_{AE}(n)$, which were independent of one another and had uniform distributions in the range of [-1;1]. $R_{MZ_C}(n)$, $R_{MA_C}(n)$, $R_{MI_C}(n)$ took new random value at each time instant n, what resulted in frequent changes of $I_C(n)$, $Z_C(n)$, however the angle of $I_C(n)$ was fixed. The series $R_{ME}(n)$, $R_{AE}(n)$, which were responsible for the shape of magnitude and angle of $E(m)$, were piecewise constant. Each of them contained only 30 random changes within whole N samples long simulation. Time points at which random changes occurred were drawn from all N possible time points. They were distributed uniformly within the whole simulation time, giving average distance of samples between consecutive random changes, which is less than estimator window length $L = 60$. In some of test cases, the magnitude of voltage E contained additional significant step distortion $S(n) = -1(n - n_1) + 1(n - n_2)$ for n_1=600, n_2=1000, where $1(n_i)$ is Heaviside step function at time instant n_i. An exemplary realization of $E(n)$ is shown in Fig. 5.
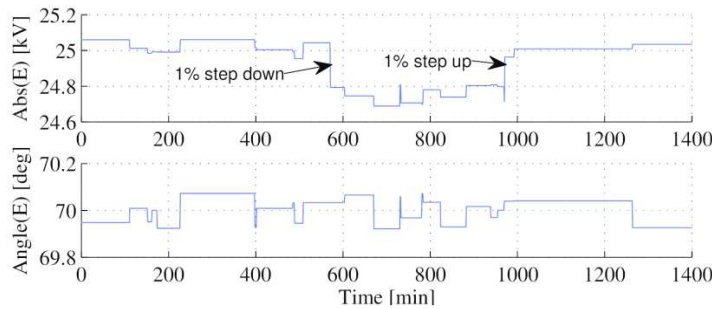

Fig. 5. Exemplary realization of $|E(n)|$ variations in VSE case.

The resulting level of variability of magnitudes and angles of $E(n)$, $Z(n)$, $I_c(n)$, $Z_c(n)$ in each test case was controlled by values of multipliers D_{MZ}, D_{AZ}, D_{MZ_c}, D_{AZ_c}, D_{MI_c}, D_{ME}, D_{SE}, D_{AE}, which scaled the depth of modulation of base magnitudes and angles.

Formulas which were used to generate complex values of grid model parameters $E(n)$, $Z(n)$, $I_c(n)$, $Z_c(n)$ are given in Tab. 1.

Table 1. Components of simulated signals.

Parameter	Magnitude [Ω, A, V]	Angle [°]
$Z(n)$	$M_Z\left(1 + D_{MZ} \cdot \sin\left(4\pi \dfrac{n}{N}\right)\right)$	$A_Z\left(1 + D_{AZ} \cdot \cos\left(4\pi \dfrac{n}{N}\right)\right)$
$Z_C(n)$	$M_{Z_C}\left(1 + D_{MZ_C} \cdot R_{MZ_C}(n)\right)$	$A_{Z_C}\left(1 + D_{AZ_C} \cdot R_{AZ_C}(n)\right)$
$I_C(n)$	$M_{I_C}\left(1 + D_{MI_C} \cdot R_{MI_C}(n)\right)$	A_{I_C}
$E(n)$	$M_E\left(1 + D_{ME} \cdot R_{ME}(n) + D_{SE} \cdot S(n)\right)$	$A_E\left(1 + D_{AE} \cdot R_{AE}(n)\right)$

Time series of complex PCC voltage $V(n)$ and complex PCC current $I(n)$ were calculated for each test case according to the assumed power system model (Fig. 1):

$$V(n) = [E(n) + I_C(n)Z(n)] \cdot \frac{Z_C(n)}{Z(n) + Z_C(n)}, \tag{17}$$

$$I(n) = [E(n) - I_C(n)Z_C(n)] \cdot \frac{1}{Z(n) + Z_C(n)}. \tag{18}$$

Each test case was a combination of the following three sub-cases:

a) Variations of background voltage $E(n)$:

CE – an ideal case of constant $E(n)$, obtained by setting $D_{ME} = 0$, $D_{SE} = 0$, $D_{AE} = 0$; the only source of errors is variability of $Z(n)$;

CSE – constant $E(n)$, except for step distortion, obtained by setting $D_{ME} = 0$, $D_{SE} = 0.01$, $D_{AE} = 0$;

VE – variable $E(n)$ containing random variations of magnitude and angle in ranges of ±0.25% M_E, ±0.5° A_E obtained by: $D_{ME} = 0.0025$, $D_{SE} = 0$, $D_{AE} = 0.5 / 360$;

VSE – variable $E(n)$, same as VE case, containing additional 1% M_E step distortion, obtained by: $D_{ME} = 0.0025$, $D_{SE} = 0.01$, $D_{AE} = 0.5 / 360$;

b) Type of grid side impedance $Z(n)$:

IZ – mainly inductive type impedance Z defined by its base phase angle: $A_Z = 70°$;

RZ – mainly resistive type impedance Z defined by its base phase angle: $A_Z = 30°$;

c) Load side variability:

HI – high load side variability defined by modulation depths of random variations of Z_c and I_c: $D_{MZ_c} = 0.2$, $D_{IZ_c} = 0.25$;

LO – low load side variability defined by modulation depths of random variations of Z_c and I_c: $D_{MZ_c} = 0.1$, $D_{MI_c} = 0.125$;

Other parameters had common values across all cases. They had base magnitudes and angles $M_E = 25\text{kV}$, $M_Z = 1\Omega$, $M_{Z_c} = 25\ \Omega$, $A_{Z_c} = 70°$, $M_{I_c} = 400\text{A}$, $A_{I_c} = 0°$ and modulation depths $D_{MZ} = 2\%$, $D_{AZ} = 5\%$, $D_{AZ_c} = 20\%$.

4.2. Evaluation of the WLS algorithm

For each test case, $R=100$ repetitions of tracking were performed. Each repetition was conducted for a different set of random series $R_{MZ_C}(n)$, $R_{MA_C}(n)$, $R_{MI_C}(n)$, $R_{ME}(n)$, $R_{AE}(n)$.

Confidence intervals, calculated for assumed extension factor $k = 2$, were validated for each realization and each time point, by checking whether true impedance value lays within confidence interval. The results $\hat{Z}(n)$ of tracking varying $Z(n)$ were delayed by the half of estimator window length L with respect to $Z(n)$ variations. Therefore, in order to eliminate the impact of that delay for confidence intervals validation, true impedance values were delayed accordingly. Taking this delay into account (shift by $L/2$ samples), confidence interval validation test condition takes the following form:

$$\hat{Z}(n) - U(n) < Z\left(n + \frac{L}{2}\right) < \hat{Z}(n) + U(n). \tag{19}$$

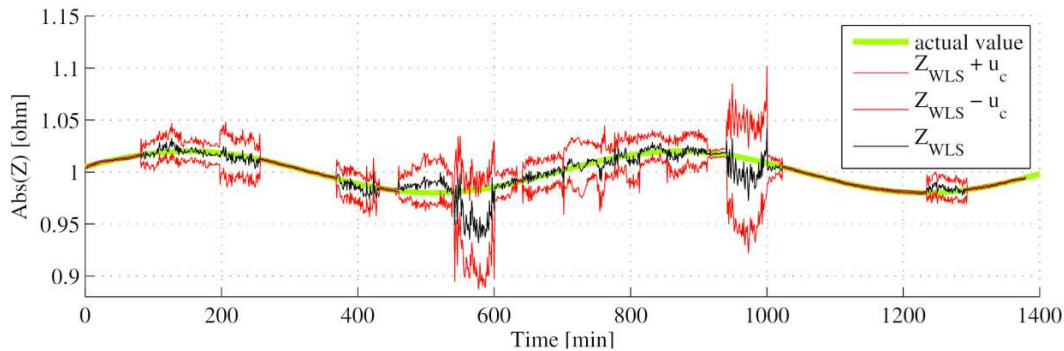The result of delaying actual impedance values by $L/2$ samples is visible in Fig. 6.

Fig. 6. Exemplary realization of impedance magnitude tracking (black) with standard uncertainty interval (red) plotted for VSE-IZ-HI case. Significant increase in uncertainty appears close to step disturbances in $|E(n)|$.

From Fig. 6 it can be seen, that impedance estimates, shifted by *L*/2 samples, are consistent with instantaneous values of actual sinusoidally varying impedance.

For each test case, the percentage number of total WLS hits, i.e. the number of true impedance values falling within confidence intervals, was calculated. WLS hits are given in Tab. 2. The hits vs time for the selected case are shown in Fig. 7.

Table 2. Relative number of WLS hits.

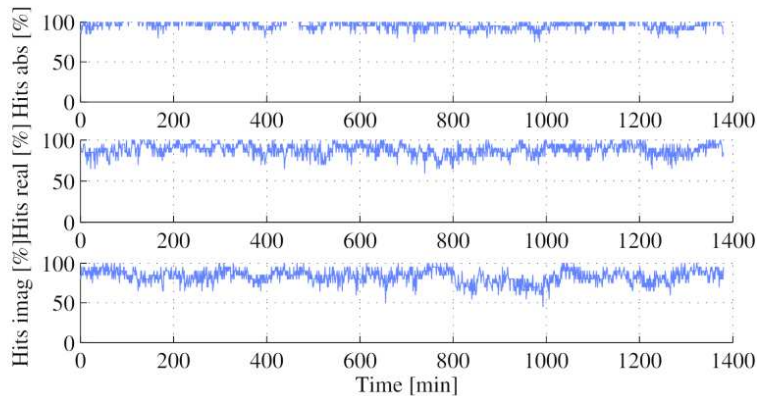| E	Z	Load var.	abs(*Z*) [%]	real(*Z*) [%]	imag(*Z*) [%]
CE	IZ	LO	99.82	98.33	97.50
		HI	98.32	92.18	89.50
	RZ	LO	99.93	95.18	98.80
		HI	99.27	82.24	94.71
CSE	IZ	LO	99.69	97.47	97.45
		HI	98.00	91.78	88.56
	RZ	LO	99.89	94.65	98.39
		HI	98.37	83.05	92.74
VE	IZ	LO	98.51	93.45	93.16
		HI	95.78	87.98	83.58
	RZ	LO	98.60	92.19	93.80
		HI	95.67	84.28	86.08
VSE	IZ	LO	98.55	93.30	93.42
		HI	95.72	88.20	83.05
	RZ	LO	98.70	92.08	93.98
		HI	95.16	84.87	85.12
Average:			97.84	89.66	91.08

Fig. 7. Percentage of hits of impedance values into confidence intervals from all realizations for VSE-IZ-HI case.

The comparison of the WLS method (10) to the LS method (7) is done by calculation of root mean squared errors (RMSE) and maximum errors (MAXE) of tracking of *Z* magnitude and angle. The errors were calculated using following formulas:

$$RMSE(\Delta) = \sqrt{\frac{1}{RN} \sum_{r=1}^{R} \sum_{n=1}^{N} |\Delta(r,n)|^2}, \tag{20}$$

$$MAXE(\Delta) = \max_r \left(\max_n |\Delta(r,n)| \right), \tag{21}$$

where $\Delta(r,n)$ could either be the error of impedance magnitude or angle estimation i.e. $\Delta(r,n) = \left| \hat{Z}(r,n) \right| - \left| Z(n) \right|$ or $\Delta(r,n) = \arg\left(\hat{Z}(r,n) \right) - \arg(Z(n))$ respectively. Index *r* denotes the number of impedance tracking repetition (realization), while index *n* denotes time within single realization. RMSE and MAXE errors are given in Tab. 3.

Table 3. Total errors of impedance magnitude and angle estimation.

Case			Magnitude				Angle			
E	Z	Load var.	RMSE [%]		MAXE [%]		RMSE [°]		MAXE [°]	
			LS	WLS	LS	WLS	LS	WLS	LS	WLS
CE	IZ	LO	0.17	0.03	0.94	0.18	0.09	0.02	0.52	0.15
		HI	0.10	0.03	0.62	0.20	0.07	0.02	0.45	0.16
	RZ	LO	0.33	0.04	2.20	0.33	0.18	0.04	1.23	0.36
		HI	0.16	0.04	1.13	0.43	0.15	0.05	1.05	0.36
CSE	IZ	LO	0.92	0.23	48.11	13.99	0.57	0.13	25.65	6.23
		HI	0.57	0.19	31.31	8.44	0.35	0.11	17.19	4.64
	RZ	LO	1.08	0.23	43.84	10.58	0.65	0.16	26.12	7.74
		HI	0.75	0.24	35.31	9.71	0.33	0.11	11.63	5.25
VE	IZ	LO	1.43	0.41	20.56	8.99	0.79	0.23	9.91	4.39
		HI	0.90	0.32	14.21	4.86	0.49	0.18	7.76	2.56
	RZ	LO	1.50	0.42	19.64	8.48	0.87	0.25	11.02	5.48
		HI	1.00	0.36	14.59	5.17	0.51	0.19	5.74	2.62
VSE	IZ	LO	2.07	0.56	45.21	12.44	1.17	0.32	24.69	6.47
		HI	1.30	0.46	25.98	11.26	0.73	0.26	16.43	6.15
	RZ	LO	2.18	0.57	42.31	11.54	1.25	0.35	26.49	7.22
		HI	1.53	0.54	31.41	12.06	0.66	0.24	11.92	4.42

4.3. Discussion of the results

It can be seen from Tab. 2 that derived confidence intervals, for empirically chosen extension factor $k = 2$, contain about 98% impedance magnitude estimates from all test cases. Even for the worst case, i.e. VSE-RZ-HI, more than 95% of magnitude estimates fit within confidence intervals. For real and imaginary part of tracked impedance, not less than 80% of results fit the intervals. It can be noticed that in general the number of hits is higher for lower load variance. It is a result of narrowing of the confidence interval with the increase of excitation level, which in this case is the variance of current I in matrix $\mathbf{X}$.

It is worth to mention, that such results are obtained using actual impedance values delayed by $L/2$, which is possible only in offline analysis, e.g. so called post-mortem analysis commonly performed after significant power grid failure. For real-time analysis, one has to accept the delay resulting in estimator bias, so the number of hits can be lower, depending on tracked impedance dynamics. Tracking delay is however an inherent feature of each other tracking estimator.

The results of comparison of the WLS and the LS shown in Tab. 3, prove that the WLS is much more accurate than the LS. Impedance tracking errors (both RMSE and MAXE) of the WLS are about 3 to 4 times smaller than those of the LS for all considered cases. An example of performance of the WLS and the LS methods is shown in Fig. 8.
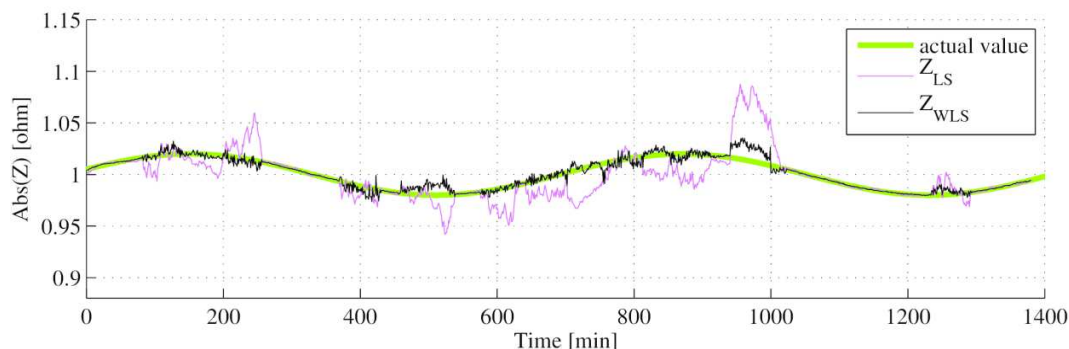

Fig. 8. Comparison of WLS and LS results for VE-IZ-HI case. The WLS method tracks varying impedance with significantly smaller errors than the LS method.

It should also be noticed, that calculated standard uncertainty $u_C(n)$ varies depending on local disturbance (see Fig. 6) and excitation level (e.g. higher load variance, better excitation, greater confidence of the result, narrower confidence interval). Thus, its values can be used to reject uncertain results.

5. Conclusion

The paper presents a new method for tracking varying grid impedance together with its confidence intervals. The robustness of the method was verified by means of simulation of 16 test cases, showing accuracy 3 to 4 times better than that of the LS [13, 30]. Estimated confidence intervals, for $k = 2$, contain about 98% of impedance magnitude estimates, even in the presence of significant background voltage variations. Thus, the proposed method can be successfully used for estimation of varying grid impedance together with its accuracy measure. Possible applications of the method are: scheduling of distributed power generation or offline (post-mortem) case study after power grid failures.

Further research plans include tracking of impedance of laboratory power system model, which has been built at AGH-UST as well as tracking of impedance of the University power grid. Additional analysis of measurement errors as well as of the background voltage distortion on the performance of the method is also planned.

Acknowledgements

References

[1] Kechroud, A., Myrzik, J. M. A., & Kling, W. L. (2009, July). A power system equivalent impedance based voltage control. In *Power & Energy Society General Meeting, 2009. PES'09. IEEE* (1−5). IEEE.

[2] Otomański, P., & Wiczyński, G. (2010, June). Search for disturbing loads in power network with the use of voltage and current fluctuation. In *Nonsinusoidal Currents and Compensation (ISNCC), 2010 International School on* (197−200). IEEE.

[3] Robert, A., et al. (1997, June). Guide for assessing the network harmonic impedance. In *Electricity Distribution. Part 1: Contributions. CIRED. 14th International Conference and Exhibition on (IEE Conf. Publ. No. 438)* (Vol. 1, 3−1). IET.

[4] Xu, W., Ahmed, E. E., Zhang, X., & Liu, X. (2002). Measurement of network harmonic impedances: practical implementation issues and their solutions. *Power Delivery, IEEE Transactions on, 17*(1), 210−216.

[5] Borkowski, D., Wetula, A., & Bien, A. (2012, July). New method for noninvasive measurement of utility harmonic impedance. In *Power and Energy Society General Meeting, 2012 IEEE* (1−8). IEEE.

[6] Cespedes, M., & Sun, J. (2012, September). Online grid impedance identification for adaptive control of grid-connected inverters. In *Energy Conversion Congress and Exposition (ECCE), 2012 IEEE* (914−921). IEEE.

[7] Staroszczyk, Z. T. (2010, September). Combined, experimental data supported simulations in development of power grid impedance identification methods. In *Harmonics and Quality of Power (ICHQP), 2010 14th International Conference on* (1−7). IEEE.

[8] Gu, H., Guo, X., Wang, D., & Wu, W. (2012, May). Real-time grid impedance estimation technique for grid-connected power converters. In *Industrial Electronics (ISIE), 2012 IEEE International Symposium on* (1621−1626). IEEE.

[9] Hoffmann, N., & Fuchs, F. W. (2012, September). Online grid impedance estimation for the control of grid connected converters in inductive-resistive distributed power-networks using extended kalman-filter. In *Energy Conversion Congress and Exposition (ECCE), 2012 IEEE* (922−929). IEEE.

[10] Arrilaga, J., & Watson, N. R. (2003). *Power system harmonics*. Chichester: John Wiley & Sons.

[11] Cobreces, S., Rodriguez, P., Pizarro, D., Rodriguez, F. J., & Bueno, E. J. (2007, June). Complex-space recursive least squares power system identification. In *Power Electronics Specialists Conference, 2007. PESC 2007. IEEE* (2478–2484). IEEE.

[12] Langella, R., & Testa, A. (2006, June). A new method for statistical assessment of the system harmonic impedance and of the background voltage distortion. In *Probabilistic Methods Applied to Power Systems, 2006. PMAPS 2006. International Conference on* (1–7). IEEE.

[13] Hui, J., Yang, H., Lin, S., & Ye, M. (2010). Assessing utility harmonic impedance based on the covariance characteristic of random vectors. *Power Delivery, IEEE Transactions on, 25*(3), 1778–1786.

[14] Kay, S. M. (1993). *Fundamentals of Statistical Signal Processing: Estimation Theory.* Englewood Clifs: Prentice Hall.

[15] Oppenheim, A. V., Schafer, R. W., & Buck, J. R. (1999). *Discrete-time signal processing* (Vol. 5). Upper Saddle River: Prentice Hall.

[16] Tarasiuk, T. (2009). Comparative study of various methods of DFT calculation in the wake of IEC Standard 61000-4-7. *Instrumentation and Measurement, IEEE Transactions on, 58*(10), 3666–3677.

[17] Duda, K. (2010). Accurate, Guaranteed Stable, Sliding Discrete Fourier Transform [DSP Tips & Tricks]. *Signal Processing Magazine, IEEE, 27*(6), 124–127.

[18] Ferrero, A., & Ottoboni, R. (1992). A low-cost frequency multiplier for synchronous sampling of periodic signals. *Instrumentation and Measurement, IEEE Transactions on, 41*(2), 203–207.

[19] Cataliotti, A., Cosentino, V., & Nuccio, S. (2007). A phase-locked loop for the synchronization of power quality instruments in the presence of stationary and transient disturbances. *Instrumentation and Measurement, IEEE Transactions on, 56*(6), 2232–2239.

[20] Zhao, Q., Hsu, Y., Guo, B., Zhao, J. (2005, June). A digital filter design for digital resampling in power system applications. *In Power and Energy Society General Meeting, 2005 IEEE* (Vol. 2, 1849–1854). IEEE.

[21] Ghadam, A. S. H., Babic, D., Lehtinen, V., & Renfors, M. (2004, May). Implementation of Farrow structure based interpolators with subfilters of odd length. In Circuits and Systems, 2004. ISCAS'04. *Proceedings of the 2004 International Symposium on* (Vol. 3, III–581). IEEE.

[22] Borkowski, D., & Bien, A. (2009). Improvement of accuracy of power system spectral analysis by coherent resampling. *Power Delivery, IEEE Transactions on, 24*(3), 1004–1013.

[23] Duda, K. (2011). DFT interpolation algorithm for Kaiser–Bessel and Dolph–Chebyshev windows. *Instrumentation and Measurement, IEEE Transactions on, 60*(3), 784–790.

[24] Liu, S. (1998, October). An adaptive Kalman filter for dynamic estimation of harmonic signals. In *Harmonics and Quality of Power Proceedings, 1998. Proceedings. 8th International Conference On* (Vol. 2, 636–640). IEEE.

[25] Dash, P. K., Pradhan, A. K., & Panda, G. (1999). Frequency estimation of distorted power system signals using extended complex Kalman filter. *Power Delivery, IEEE Transactions on, 14*(3), 761–766.

[26] Karimi-Ghartemani, M., & Iravani, M. R. (2005). Measurement of harmonics/inter-harmonics of time-varying frequencies. *Power Delivery, IEEE Transactions on, 20*(1), 23–31.

[27] Pintelon, R., & Schoukens, J. (2004). *System identification: a frequency domain approach.* John Wiley & Sons.

[28] Wu, W. B., & Xiao, H. (2012). Covariance Matrix Estimation in Time Series. *Handbook of Statistics, Vol. 30: Time Series Analysis: Methods and Applications*, 187–209.

[29] Joint Committee for Guides in Metrology (2008). JCGM 100: Evaluation of measurement data - guide to the expression of uncertainty in measurement, *JCGM, Tech. Rep.*, 2008.

[30] Borkowski, D. (2013, September). Power system impedance tracking using sliding, finite memory complex recursive least squares. In *Proceedings of 17th IEEE Conference Signal Processing: Algorithms, Architectures, Arrangements, and Applications*. IEEE.